RESEARCH ARTICLE | MAY 21 2026

Near-constant thermoelectric power factor of GaN two-dimensional hole gas in cryogenic environments

Special Collection: Frontiers in Nitride Semiconductors Research

Lex Pardon ; Diana C. Leitao ; Filipe A. Cardoso ; Karen M. Dowling

Appl. Phys. Lett. 128, 202107 (2026)
https://doi.org/10.1063/5.0324609

Applied Physics Letters ARTICLE pubs.aip.org/aip/apl

Near-constant thermoelectric power factor of GaN two-dimensional hole gas in cryogenic environments

Cite as: Appl. Phys. Lett. **128**, 202107 (2026); doi: 10.1063/5.0324609
Submitted: 26 January 2026 · Accepted: 4 May 2026 ·
Published Online: 21 May 2026

Lex Pardon,[1] Diana C. Leitao,[2] Filipe A. Cardoso,[1] and Karen M. Dowling[1,a)]

AFFILIATIONS

[1]Department of Microelectronics, Delft University of Technology, Delft, The Netherlands
[2]Department of Applied Physics, Eindhoven University of Technology, Eindhoven, The Netherlands

Note: This paper is part of the Special Topic on Frontiers in Nitride Semiconductors Research.
[a)]**Author to whom correspondence should be addressed:** K.M.Dowling@tudelft.nl

ABSTRACT

This work investigates the thermoelectric properties of a gallium nitride (GaN)-based two-dimensional hole gas (2DHG) using a double heterojunction, which can be utilized in complementary GaN thermoelectric (TE) platforms for power generation in extreme environments. A 5×10^{12} cm^{-2} hole density, a Hall mobility of up to 20 cm^2 V^{-1} s^{-1}, and a Seebeck coefficient of 0.4mVK^{-1} have been measured, resulting in a power factor of 0.5–1.0mWm^{-1} K^{-2} over a 300–77 K temperature range. These results demonstrate the stability and usability of the thermoelectric properties of GaN using hole conduction at sub-100 K temperatures, therefore providing clear evidence that GaN-based 2DHGs can function as a stable cryogenic TE platform, opening new opportunities for complementary device architectures (leveraging both 2DHGs for p-type and two-dimensional electron gases for n-type) optimized for extreme environment electronics commonly encountered in deep-space missions, where other materials become unreliable.

Thermoelectric (TE) materials are used in thermoelectric generators (TEGs), which are typically bench-marked with the zT figure of merit. This zT has two key components, the power factor (PF) and thermal conductivity (k), scaled by the applied thermal difference (ΔT). While previous work has shown reducing k can improve zT, this strategy is hitting practical and theoretical limits in most material systems.[1] Furthermore, recent research in thin-film-based TE materials show improved efficiency for electric power generation, as the correlation between k and PF can be decoupled.[2] Therefore, the PF should be increased, which is determined using $PF = S^2\sigma$, where S represents the Seebeck coefficient and σ the electrical conductivity. State-of-the-art p-type Sb_2Te_3 thin films have recently demonstrated competitive room-temperature performance, achieving power factors as high as 1.94mWm^{-1} K^{-2}, yet these studies remain focused on room-temperature and above,[3] leaving their behavior and stability in cryogenic regimes largely unexplored. Moreover, bulk TE materials are dominated by Bismuth-based materials, such as p-type doped $CsBi_2Te_3$ and $Bi_{2-x}Ca_xSe_3$ alloys, due to their high room-temperature PF of up to 5 and 0.8mWm^{-1} K^{-2}, respectively.[4,5] These materials rely on heavy doping to achieve optimal carrier concentrations, making them susceptible to carrier freeze out at cryogenic temperatures, which leads to reduced PF as well. For example, the PF of $CsBi_2Te_3$ falls below 1mWm^{-1} K^{-2} at 150 K.[4] This freeze out behavior limits the ability of doped TE platforms to maintain performance across a broad temperature range, particularly in cryogenic environments.[6] In addition, integrating these materials into micro-TEG platforms remains challenging, as their deposition, doping profiles, and packaging requirements are often incompatible with standard IC fabrication workflows.

Gallium nitride (GaN), known for its wide bandgap and temperature-independent polarization-induced carrier formation, provides a reliable platform in both cryogenic and high-temperature operation.[7] Its intrinsic polarization limits carrier freeze out, ensuring reliable performance at temperatures as low as tens of Kelvin since it does not rely as heavily on dopant activation.[8] Earlier works have investigated the thermoelectric properties of AlGaN/GaN two-dimensional electron gases (2DEGs), where a constant PF of 4–7mWm^{-1} K^{-2} was measured at temperatures of 50–300 K,[9–11] in

which a significant increase in the PF due to phonon-drag has been measured.[12]

Beyond the extensively studied 2DEGs, recent work has demonstrated that polarization-induced GaN/AlGaN heterostructures can also support high-density two-dimensional hole gases (2DHGs), with sheet densities exceeding $10^{13}\,\mathrm{cm}^{-2}$ at cryogenic temperatures.[13,14] Additionally, GaN is inherently well-suited for monolithic integration, enabling the seamless co-fabrication of diverse high-performance electronic and optoelectronic devices on a single chip. Double-heterojunction designs have been shown to simultaneously host a 2DHG and a complementary 2DEG, whilst being isolated,[14] providing a robust platform for complementary 2DHG and 2DEG studies. Despite these advances, the thermoelectric properties such as S and PF of GaN 2DHGs have not yet been experimentally characterized. In contrast to the well-studied cryogenic behavior of 2DEG-based TEGs, the thermoelectric response of GaN 2DHG devices remains largely unexplored, despite their potential for enabling highly efficient complementary micro-TEGs.[15] This work investigates the TE properties of a 2DHG as a p-type GaN thermoelectric material, allowing the use of complementary micro-TEGs in cryogenic environments. This approach enables more efficient power generation in harsh environments, such as those encountered by rovers or satellites in outer space.

A GaN double-heterojunction structure supporting both a 2DHG and a complementary 2DEG was grown using metal–organic chemical vapor deposition (MOCVD) by Dowa Electronics Materials Co., Ltd. The stack consists of a GaN/AlGaN/GaN/p-GaN double heterojunction, as shown in Fig. 1(a). The 30 nm thick top p-GaN layer is doped with a $3 \times 10^{19}\,\mathrm{cm}^{-3}$ magnesium concentration to elevate the valence band as seen in Fig. 1(b), promoting the formation of a 2DHG in the 20 nm thick unintentionally doped GaN layer.[14] The Mg-doped p-GaN also reduces the Schottky barrier height, enabling low-resistance Ohmic contacts.[16,17]

The AlGaN layer is carefully chosen to optimize the PF of the 2DHG, as determined through Schrödinger–Poisson-based simulations using Nextnano[18] in combination with S and mobility estimation models. By adjusting the aluminum (Al) content (x) in the $Al_xGa_{1-x}N$ barrier, the sheet hole density of the 2DHG (p_s) can be effectively controlled. Increasing the Al content results in higher 2DHG densities, which enhances the conductivity of the 2DHG. The conductivity can be estimated using

$$\sigma = q p_s \mu_h, \tag{1}$$

where q is the elementary charge and μ_h is the mobility of holes in the 2DHG.

The Seebeck coefficient of solely the 2DHG in this stack can be estimated using

$$S = -\frac{1}{qT}\frac{\int (E - |E_v - E_F|)\sigma(E)\,dE}{\int \sigma(E)\,dE}, \tag{2}$$

where T is the absolute temperature, $\sigma(E)$ is the differential conductivity of holes, and $|E_v - E_F|$ represents the energy difference between the valence band edge and the Fermi level extracted from Nextnano[18] simulations. Whenever the sheet density is increased by raising the Al content (x), the semiconductor becomes more degenerate, increasing $|E_v - E_F|$, which reduces S. This highlights the trade-off in selecting x, where higher Al content not only increases conductivity through a larger hole density but also decreases S, which together determine the achievable PF. An Al content of $x = 0.2$ was chosen to provide an optimal balance between achieving a high PF and maintaining practical feasibility, considering the maximum possible stress in the layer. The AlGaN layer thickness was determined to ensure the polarization of the 2DHG within the u-GaN layer using Nextnano,[18] whilst being limited by the maximum thickness to prevent detrimental cracking during epitaxy.

Under the polarizing $Al_{0.2}Ga_{0.8}N$ layer, a 1 μm thick unintentionally doped Gan (u-GaN) layer is located, in which a 2DEG is formed through similar polarizing effects of the AlGaN layer. The 2DEG electron density is expected to match the 2DHG density according to Nakajima *et al.*[19] and estimated using Nextnano.[18]

A Ni 20 nm/Au 20 nm metal contact layer was deposited on the p-GaN surface by physical vapor deposition and patterned using a lift-off process to create electrical contacts to the 2DHG. The contacts were annealed at 550 °C for 20 min in ambient air to promote low-resistance p-type tunneling-contact behavior.[16,17] Two different device structures were fabricated to enable thermoelectric characterization. Configuration 1 uses $25 \times 5\,\mathrm{mm}^2$ dies with metal contacts deposited at both ends, designed to mount onto a printed circuit board (PCB) to measure S. Configuration 2 uses $10 \times 10\,\mathrm{mm}^2$ dies featuring four $1 \times 1\,\mathrm{mm}^2$ corner contacts, which are used to form van der Pauw geometries for measuring sheet resistance (configuration 2a), Hall mobility, and sheet hole density (configuration 2b) of the isolated 2DHG.

The Seebeck coefficient was measured using configuration 1, a cantilever PCB mounted on a cryocooler as seen in Fig. 2, where seven individual samples from the same wafer were fabricated and thermally mounted between a cold copper-mounted section and a resistively heated hot section, mechanically isolated by a long thermal path. Silicon diode temperature sensors on both sides are used to measure a temperature difference of up to 10 K and average sample temperatures between approximately 65 and 300 K, ensuring reliable characterization. The generated Seebeck voltage across the semiconductor strip is measured to determine S using $S(T_{\mathrm{avg}}) = -\frac{\Delta V}{\Delta T}$, with error bars

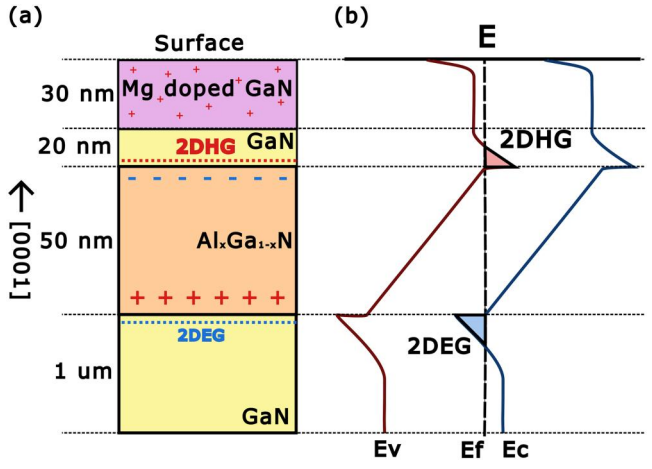

FIG. 1. (a) Schematic drawing of the 2DHG double heterojunction (not to scale) and (b) its energy band diagram.

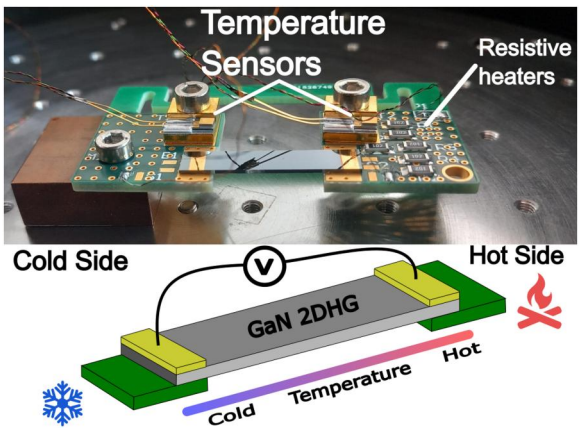

FIG. 2. Photograph and pictogram of diving-plank setup with GaN die (configuration 1) mounted on a PCB with thermal isolation to perform Seebeck coefficient measurements.

describing the standard error of the mean between seven individual measured samples. A positive S has been measured [Fig. 3(a)], indicating that the majority charge carriers are holes. To confirm that S originates from the 2DHG rather than the p-GaN capping layer, the impact of the p-GaN layer to the S measurements is estimated using

$$S_t = \frac{\Sigma_i S_i \sigma_i}{\sum_i \sigma_i}, \tag{3}$$

where S and the conductivity (σ) of parallel TE materials can be used to determine the total S or the impact of a singular layer to the complete stack. Using Eq. (3), the impact of the top p-GaN layer compared to the 2DHG is estimated to be 2% at 300 K, decreasing to a negligible impact (<0.1%) at 200 K and below. Furthermore, according to Brandt *et al.*,[21] S of the p-GaN layer is expected to have a strong temperature dependence, converging toward zero, and even reverses polarity below 120 K due to Mg-acceptor freeze out, which is not observed in this work. This indicates that the p-GaN layer's contribution was negligible. S obtained in this work remains constant across the measured temperature range, showing no polarity inversion or decrease at low temperatures, confirming this theory. These different behaviors and estimations suggest that the performed measurement is primarily influenced by the 2DHG contribution, rather than the p-GaN layer.

The simulated S is estimated using Eq. (2) and Nextnano[18] to determine the energy levels of the 2DHG. The effective hole mass of the 2DHG is to be expected between $0.5m_e$ and $2.5m_e$,[22] resulting in a higher S compared to the much lower effective electron mass of 2DEGs as seen in Fig. 3(a). The measured S aligns closely with the simulated trend, increasing with temperature at the same rate, while the measured values remain marginally higher. At colder sub-100 K temperatures, the measured data show a noticeable boosting effect that does not appear in the simulations. This effect is accompanied by an increase in the standard error of the mean, which could be caused by tensile strain induced by differential thermal expansion rates of the sample and PCB or could be more fundamental, such as phonon-drag. For comparison, the results of two 2DEG systems are presented, featuring thick (1.2 μm) and thin (150 nm) u-GaN layers. The thick u-GaN sample shows a similar boosting effect at lower temperatures, as phonon-drag is more pronounced compared to the thin GaN samples.[12] Confirming and individually separating the different boosting

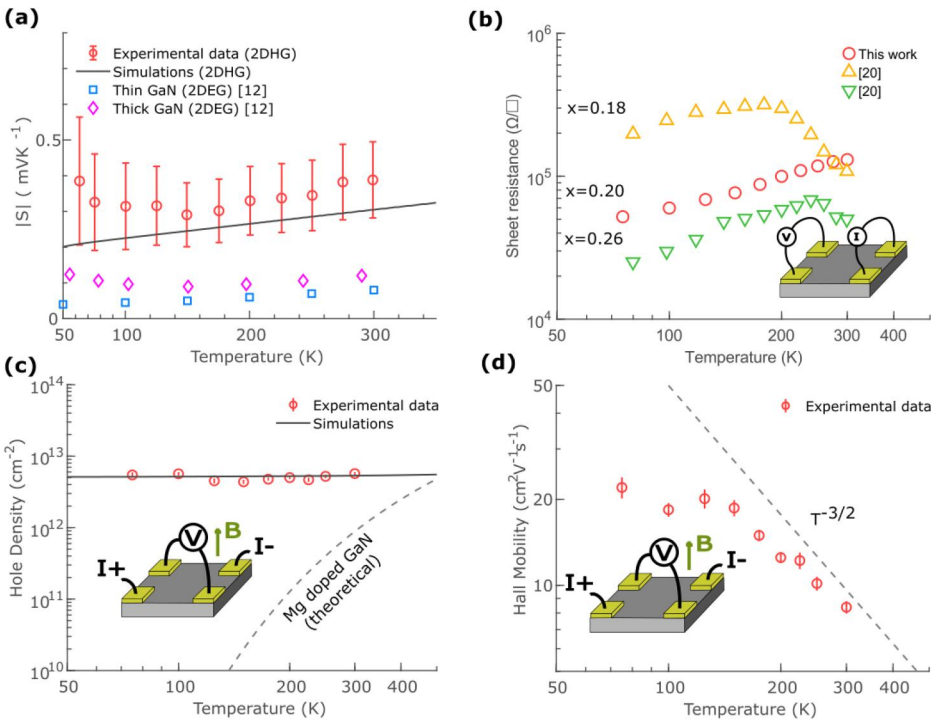

FIG. 3. Material characterization results of the 2DHG GaN thermo-electrical devices, including the (a) Seebeck coefficient using configuration 1, (b) sheet resistance including state-of-the-art comparison with results,[20] including an insert of configuration 2a, (c) hole density, and (d) hole mobility over 77–300 K, with drawings of van der Pauw structures (configuration 2b) used to determine the sheet density and hall mobility using a 594 mT magnetic field.

effects at low temperature, such as phonon-drag contributions to the 2DHG and the influence of added tensile strain, would require more detailed measurements, such as on-chip measurement structures, to avoid the need for an external PCB equipped with heaters and temperature sensors to avoid thermally induced tensile strain, or varying different structure compositions, which lie outside the scope of this work. The sheet resistance is measured using configuration 2a and is plotted in Fig. 3(b), the hole mobility and sheet hole density measurements were measured using configuration 2b and are plotted in Figs. 3(c) and 3(d). The sheet resistance, hole mobility, and hole sheet density measurements were performed in a liquid nitrogen-cooled cryostat for low-temperature control.

At room temperature, the 2DHG shows a sheet resistance of 131 kΩ/□, falling to 52 kΩ/□ when cooled to 77 K, showing metallic behavior commonly seen in two-dimensional carrier gasses. Figure 3(b) compares the temperature-dependent sheet resistance of 2DHGs of similar double-heterostructures with different Al contents in the AlGaN barrier. The 2DHG measured in this work ($x = 0.2$) exhibits a sheet resistance that falls between previously reported structures with $x = 0.18$, which has a higher resistance, and $x = 0.26$, which has a lower resistance.[20] This trend is consistent with the expected increase in hole sheet density with higher Al content, resulting in lower sheet resistance. Additionally, previously reported structures by Shao *et al.*,[20] shown in Fig. 3(b), use a three times thicker and partially heavier doped (5×10^{19} cm^{-3}) p-GaN capping layers, resulting in a transition between approximately 180 and 230 K from low-temperature metallic, 2DHG dominated transport to high-temperature thermally activated hole conduction. The structure in this work uses a thinner p-GaN capping layer, leading to a much weaker contribution from the p-GaN layer. As a result, a similar transition is expected to occur at a significantly higher temperature, estimated to be around 325 K, and therefore lies outside the temperature range investigated in this study.

Hall measurements were carried out using a 594 mT magnetic field to determine the sheet density and hole mobility. Figure 3(c) plots the 2DHG sheet density over temperature, where the sheet hole density is measured to be $5 \times 10^{12} \pm 11\%$ cm^{-2} over a temperature range of 77–300 K. The experimental results are consistent with simulations performed by Nextnano,[18] indicating that no freeze out occurs at lower temperatures. Additionally, the Hall-voltage polarity confirms that the majority carriers are holes, demonstrating that only the 2DHG is contacted. Furthermore, an estimate of the top-layer p-GaN hole concentration (p_{mg}) is plotted using

$$p_{mg} \approx t_{pGaN} \cdot \sqrt{N_A \frac{N_V}{g_A} \exp\left(\frac{-E_A}{k_B T}\right)}, \tag{4}$$

where t_{pGaN} is the p-GaN layer thickness, $N_A = 3 \times 10^{19}$ cm^{-3} is the Mg concentration, N_V is the effective density of states at the valence band edge, $g_A = 4$ represents the acceptor degeneracy factor of GaN, and $E_A = 168$ meV the activation energy of the Mg dopants.[20] This estimation of the sheet hole density of the p-GaN layer at cryogenic temperatures is several orders of magnitude lower than the experimentally measured values, indicating that the Mg-doped p-GaN layer does not significantly contribute to the measured sheet hole density and is effectively temperature-independent.

Figure 3(d) shows the measured Hall mobility of the 2DHG, with 8 cm^2/Vs at 300 K, initially increasing at a temperature dependent slope of $T^{-3/2}$, indicating that acoustic phonon scattering is dominant until the hole mobility saturates at 20 cm^2 V^{-1} s^{-1} at 150 K and below, becoming temperature independent, commonly seen in similar 2DHG structures.[23]

While the individually measured thermoelectric properties provide an in-depth insight into the formed 2DHG, the PF combines the individual measurements into a single performance indicator. The PF is evaluated using

$$PF = \frac{S^2}{t \cdot R_{sh}}, \tag{5}$$

where S is the measured Seebeck coefficient, R_{sh} is the sheet resistance, and t is the effective thickness of the 2DHG. The 2DHG thickness is extracted from Nextnano band diagram simulations, in which the Fermi level is lower than the valence band. Using this method, t is determined to be 1.4 nm at 50 K and 0.5 nm at 300 K. In order to make a fair, conservative, comparison with other non-polarizing TE materials, t is assumed to be 2 nm over the complete temperature range of this work while the PF is determined.

Figure 4 shows the derived PF of the measured 2DHG to be 0.5 mWm^{-1} K^{-2} at 300 K, increasing to 1 mWm^{-1} K^{-2} at 77 K, because S increases and resistivity decreases with lower temperatures. Overall, the PF of the GaN 2DHG remains extremely constant over a temperature range of 77–300 K, unlike bulk Mg-doped p-GaN,[21] where carrier freeze out significantly decreases performance at lower temperatures. While the Bi-based materials initially outperform the presented GaN sample in typical temperatures, all three reference materials experience a substantial decrease in their PF as temperature decreases.[4,5] In contrast, the GaN-based sample maintains a nearly constant, even increasing PF over the entire temperature range. Moreover, the 2DHG surpasses the state-of-the-art BiCaSe in PF below approximately 100 K, demonstrating its low-temperature stability and potential for cryogenic thermoelectric applications over other materials. While this work determined the PF of the generated 2DHG, previous studies suggest that superlattice structures can further enhance the lateral power

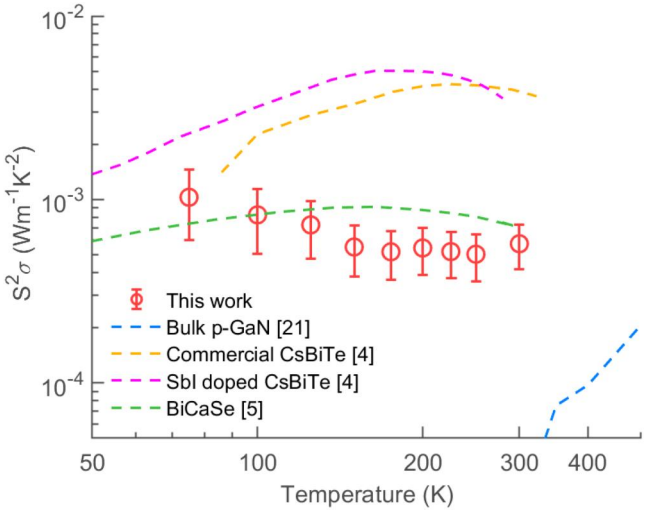

FIG. 4. Plot of determined PF of GaN 2DHG, including comparison to recent Bi-based p-type TEG materials and bulk Mg-doped GaN.[4,5,21]

density.[24,25] Exploring such superlattice-based approaches therefore represents a promising direction for future improvement.

This work presents the first measurements of the TE properties of a double heterostructure-based 2DHG in GaN, enabling the use of complementary n- and p-type TEGs based on GaN. A Seebeck coefficient of 0.3–0.4 mV K^{-1}, a sheet resistance of 131–52 kΩ/□ with a sheet hole density of 5×10^{12} cm^{-2} and a mobility of 8–20 cm^2 V^{-1} s^{-1}, resulted in a stable PF of 0.5–1 mW m^{-1} K^{-2} over a temperature range of 70–300 K. This work is a key step toward the use of complementary GaN micro-TEGs[15] more suited for reliable on-chip power delivery in extreme conditions, including cryogenic and deep-space environments.

The devices were fabricated in Kavli Nanolab and the Else Kooi Laboratory (EKL) at TU Delft. The authors acknowledge Lukasz Pakula and Jeroen Francke of the Electronic Instrumentation Lab at TU Delft and the Physics of Nanostructures Lab at TU Eindhoven for their support and assistance with the experimental equipment and setups. This work was supported by Delft University of Technology under the Delft Technology Fellowship.

AUTHOR DECLARATIONS

Conflict of Interest

The authors have no conflicts to disclose.

Author Contributions

Lex Pardon: Data curation (equal); Formal analysis (equal); Investigation (equal); Methodology (equal); Software (equal); Validation (equal); Visualization (equal); Writing – original draft (equal). **Diana C. Leitao:** Resources (equal); Validation (equal); Visualization (equal); Writing – review & editing (equal). **Filipe A. Cardoso:** Methodology (equal); Project administration (equal); Supervision (equal); Writing – review & editing (equal). **Karen M. Dowling:** Conceptualization (equal); Funding acquisition (equal); Investigation (equal); Methodology (equal); Resources (equal); Supervision (equal); Validation (equal); Writing – review & editing (equal).

DATA AVAILABILITY

The data that support the findings of this study are available within the article, and the data that support the findings of this study are available from the corresponding author upon reasonable request.

REFERENCES

[1]A. Mehdizadeh Dehkordi, M. Zebarjadi, J. He, and T. M. Tritt, "Thermoelectric power factor: Enhancement mechanisms and strategies for higher performance thermoelectric materials," Mater. Sci. Eng., R **97**, 1–22 (2015).
[2]X. Chen, Z. Zhou, Y.-H. Lin, and C. Nan, "Thermoelectric thin films: Promising strategies and related mechanism on boosting energy conversion performance," J. Materiomics **6**, 494–512 (2020).
[3]Y. L. Li, W. Y. Yang, Y. M. Peng, J. M. Yao, Y. M. Zhong, Z. L. Zhang, M. Wei, G. X. Liang, P. Fan, and Z. H. Zheng, "Optimized thermoelectric properties of flexible p-type Sb_2Te_3 thin film prepared by a facile thermal diffusion method," J. Alloys Compd. **948**, 169730 (2023).
[4]D.-Y. Chung, T. P. Hogan, M. Rocci-Lane, P. Brazis, J. R. Ireland, C. R. Kannewurf, M. Bastea, C. Uher, and M. G. Kanatzidis, "A new thermoelectric material: $CsBi_4Te_6$," J. Am. Chem. Soc. **126**, 6414–6428 (2004).
[5]Y. S. Hor, A. Richardella, P. Roushan, Y. Xia, J. G. Checkelsky, A. Yazdani, M. Z. Hasan, N. P. Ong, and R. J. Cava, "p-type Bi_2Se_3 for topological insulator and low-temperature thermoelectric applications," Phys. Rev. B **79**, 195208 (2009).
[6]N. Zulkepli, J. Yunas, M. A. Mohamed, and A. A. Hamzah, "Review of thermoelectric generators at low operating temperatures: Working principles and materials," Micromachines **12**, 734 (2021).
[7]A. J. Suria, A. S. Yalamarthy, H. So, and D. G. Senesky, "DC characteristics of ALD-grown Al_2O_3/AlGaN/GaN MIS-HEMTs and HEMTs at 600 °C in air," Semicond. Sci. Technol. **31**, 115017 (2016).
[8]O. Ambacher, R. Dimitrov, M. Stutzmann, B. E. Foutz, M. J. Murphy, J. A. Smart, J. R. Shealy, N. G. Weimann, K. Chu, M. Chumbes, B. Green, A. J. Sierakowski, W. J. Schaff, and L. F. Eastman, "Role of spontaneous and piezoelectric polarization induced effects in group-III nitride based heterostructures and devices," Phys. Status Solidi B **216**, 381–389 (1999).
[9]A. S. Yalamarthy, H. So, M. Muñoz Rojo, A. J. Suria, X. Xu, E. Pop, and D. G. Senesky, "Tuning electrical and thermal transport in AlGaN/GaN heterostructures via buffer layer engineering," Adv. Funct. Mater. **28**, 1705823 (2018).
[10]C. Bryan, P. Faucherand, M. Charles, M. Plissonnier, and G. Savelli, "Thermoelectric properties of n-type GaN and 2D electron gas in AlGaN-GaN heterostructure," J. Electron. Mater. **50**, 1301–1306 (2021).
[11]H. Ohta, S. W. Kim, S. Kaneki, A. Yamamoto, and T. Hashizume, "High thermoelectric power factor of high-mobility 2D electron gas," Adv. Sci. **5**, 1700696 (2018).
[12]A. S. Yalamarthy, M. Muñoz Rojo, A. Bruefach, D. Boone, K. M. Dowling, P. F. Satterthwaite, D. Goldhaber-Gordon, E. Pop, and D. G. Senesky, "Significant phonon drag enables high power factor in the AlGaN/GaN two-dimensional electron gas," Nano Lett. **19**, 3770–3776 (2019).
[13]R. Chaudhuri, S. J. Bader, Z. Chen, D. A. Muller, H. G. Xing, and D. Jena, "A polarization-induced 2D hole gas in undoped gallium nitride quantum wells," Science **365**, 1454–1457 (2019).
[14]A. Nakajima, Y. Sumida, M. H. Dhyani, H. Kawai, and E. M. Narayanan, "High density two-dimensional hole gas induced by negative polarization at GaN/AlGaN heterointerface," Appl. Phys. Express **3**, 121004 (2010).
[15]Q. Zhang, K. Deng, L. Wilkens, H. Reith, and K. Nielsch, "Micro-thermoelectric devices," Nat. Electron. **5**, 333 (2022).
[16]D. Mistele, F. Fedler, H. Klausing, T. Rotter, J. Stemmer, O. K. Semchinova, and J. Aderhold, "Investigation of Ni/Au-contacts on p-GaN annealed in different atmospheres," J. Cryst. Growth **230**, 564–568 (2001).
[17]J. K. Ho, C. S. Jong, C. C. Chiu, C. N. Huang, C. Y. Chen, and K. K. Shih, "Low-resistance ohmic contacts to p-type GaN," Appl. Phys. Lett. **74**, 1275–1277 (1999).
[18]S. Birner, T. Zibold, T. Andlauer, T. Kubis, M. Sabathil, A. Trellakis, and P. Vogl, "Nextnano: General purpose 3-D simulations," IEEE Trans. Electron Devices **54**, 2137–2142 (2007).
[19]A. Nakajima, P. Liu, M. Ogura, T. Makino, S. I. Nishizawa, S. Yamasaki, H. Ohashi, K. Kakushima, and H. Iwai, "Temperature-independent two-dimensional hole gas confined at GaN/AlGaN heterointerface," Appl. Phys. Express **6**, 091002 (2013).
[20]P. Shao, X. Fan, S. Li, S. Chen, H. Zhou, H. Liu, H. Guo, W. Xu, T. Tao, Z. Xie, H. Lu, K. Wang, B. Liu, D. Chen, Y. Zheng, and R. Zhang, "High density polarization-induced 2D hole gas enabled by elevating Al composition in GaN/AlGaN heterostructures," Appl. Phys. Lett. **122**, 142102 (2023).
[21]M. S. Brandt, P. Herbst, H. Angerer, O. Ambacher, and M. Stutzmann, "Thermopower investigation of n- and p-type GaN," Phys. Rev. B **58**, 7786–7791 (1998).
[22]J. Wang, D. G. Rickel, C. F. C. Chang, Z. Zhang, P. Peng, Y. Huang, A. K. Azad, D. Jena, H. G. Xing, and S. A. Crooker, "THz cyclotron resonance of a 2D hole gas in a GaN/AlN heterostructure," Appl. Phys. Lett. **126**, 213102 (2025).
[23]Y. H. Ng, Z. Zheng, L. Zhang, R. Liu, T. Chen, S. Feng, Q. Shao, and K. J. Chen, "Distribution and transport of holes in the p-GaN/AlGaN/GaN heterostructure," Appl. Phys. Lett. **123**, 142106 (2023).
[24]A. Sztein, J. E. Bowers, S. P. Denbaars, and S. Nakamura, "Polarization field engineering of GaN/AlN/AlGaN superlattices for enhanced thermoelectric properties," Appl. Phys. Lett. **104**, 42106 (2014).
[25]Y. Uematsu, T. Ishibe, T. Mano, A. Ohtake, H. T. Miyazaki, T. Kasaya, and Y. Nakamura, "Anomalous enhancement of thermoelectric power factor in multiple two-dimensional electron gas system," Nat. Commun. **15**, 322 (2024).